

## PROPERTIES OF FINAL STATES IN pp AND pn INTERACTIONS\*

BY D. K. BHATTACHARJEE AND T. ROY

High Energy Physics Division, Department of Physics, Jadavpur University, Calcutta\*\*

*(Received June 18, 1982)*

Properties of pp and pn multiplicity distributions are analysed within the momentum range 100–400 GeV/c. The pp and pn distributions at 400 GeV/c were extracted through an empirical model from the pd interaction data at 400 GeV/c. The different significant parameters are derived and consequences discussed.

PACS numbers: 13.85.-t

*1. Introduction*

Recent interest on deuterium target has grown mainly because of the availability of neutron target, which has become important for the testing of the predictions of quark-parton model and the like. In the recent past a number of experiments were performed on the interactions of proton at various momenta with deuterium in bubble chamber. Though the method of extraction of pp and pn multiplicity distributions and the analysis followed a more or less general pattern, they differed in some details. It would therefore be worth while to look into the general pattern of extracted pp and pn distributions and the comparison of the pp distributions extracted from pd experiments with those from hydrogen Bubble chamber experiments which has not yet been reported.

In the first part of the paper we report on the data obtained from the scanning of pictures of the 30 inch deuterium bubble chamber experiment at 400 GeV/c incident proton momentum performed at FNAL and the method for the extraction of pp and pn multiplicity distributions. We then compare the results with those obtained in other deuterium and hydrogen bubble chamber experiments.

*2. 400 GeV pd data and method of analysis*

All measurements were made for charged multiplicities  $N_{ch} \geq 3$ . Approximately 75% of the pictures are double scanned. The scanning efficiency for the double scanned events was  $99 \pm 1\%$  independent of multiplicity. The sample of events included a total of 49940

\* A modified version of the paper contributed at the EPS Int. Conf. on H. E. Phys., Lisbon, July 1981.

\*\* Address: Department of Physics, Jadavpur University, Calcutta-700 032, India.

beam tracks and a total of 5188 events. The resulting multiplicity distribution after all “standard” and spectator corrections is shown in Fig. 1, and are given in Table I. To correct for the double scattering within deuterium, and for extracting the pp and pn distributions, we have employed a semi-empirical model. This model takes into account the assumption that the final state is achieved in a distance smaller than the inter-nucleon

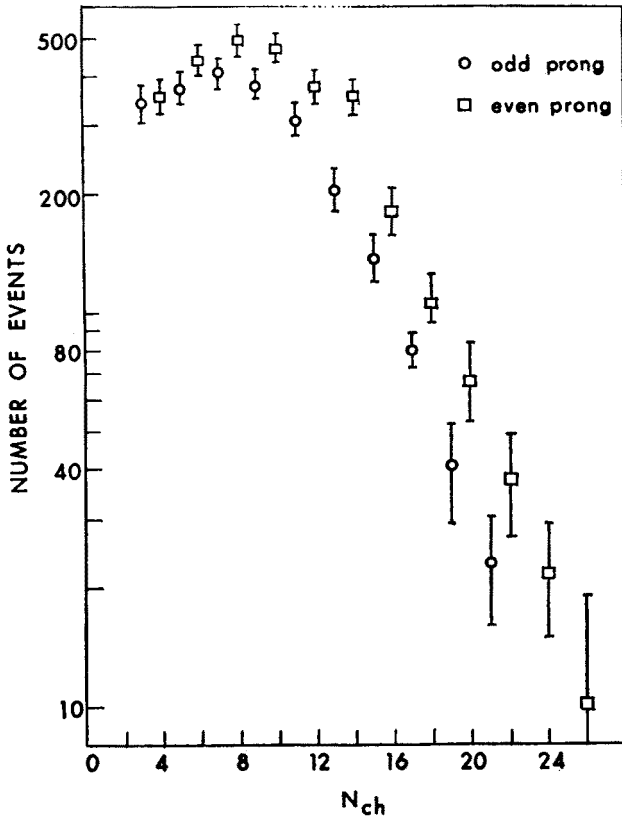


Fig. 1. Odd- and even prong multiplicity distribution from pd interaction at 400 GeV/c (Data from Col. 6, Table I)

spacing within deuterium and there is an equal probability for each particle (including neutrals) produced in the first interaction to interact with the second nucleon. Following assumptions are used in the double scattering model:

- (1) The number  $n_0$  of neutrals produced in the first interaction is given by  $n_0 = n_-$  for pp interactions and  $n_0 = n_- + 1$  for pn interactions.
- (2) The multiplicity distribution of the second scattering events induced by a charged particle (or neutral) from the first interaction is the same as that of the observed secondary interactions (or interactions induced by neutrals) in the chamber and it depends on the multiplicity of the first interaction.

The probability  $\alpha$  of a double scattering event having an initial  $i$ -prong interaction

TABLE I

Charged-multiplicity distribution in pd interactions at 400 GeV/c

$N_{\text{ch}}$	Scanned events	Contribution from assigned multiplicity	Events after corrections	Corrected events
3	230	9	$261 \pm 25$	$347 \pm 34$
4	401	14	$444 \pm 32$	$358 \pm 35$
5	305	28	$346 \pm 30$	$375 \pm 33$
6	440	26	$473 \pm 29$	$444 \pm 36$
7	341	36	$383 \pm 25$	$404 \pm 33$
8	483	34	$519 \pm 27$	$498 \pm 41$
9	315	44	$364 \pm 23$	$383 \pm 33$
10	430	51	$487 \pm 32$	$468 \pm 37$
11	252	47	$274 \pm 24$	$311 \pm 31$
12	342	60	$412 \pm 29$	$374 \pm 33$
13	178	36	$194 \pm 19$	$203 \pm 26$
14	196	84	$275 \pm 29$	$265 \pm 31$
15	94	25	$101 \pm 14$	$138 \pm 18$
16	106	119	$219 \pm 22$	$181 \pm 25$
17	63	12	$68 \pm 7$	$80 \pm 8$
18	49	75	$118 \pm 16$	$106 \pm 20$
19	29	9	$31 \pm 5$	$41 \pm 11$
20	35	49	$79 \pm 14$	$68 \pm 15$
21	15	5	$17 \pm 5$	$23 \pm 7$
22	20	27	$44 \pm 3$	$38 \pm 11$
23	4	3	$5 \pm 1$	$5 \pm 3$
24	9	19	$22 \pm 7$	$22 \pm 7$
25	2	1	$3 \pm 3$	$6 \pm 3$
26	2	17	$14 \pm 0$	$10 \pm 7$
27	2	1	$1 \pm 0$	$1 \pm 0$
28	1	6	$5 \pm 3$	$5 \pm 3$
29	1	0	0	0
30	1	0	$1 \pm 0$	$1 \pm 0$
Odd	1831	256	$2048 \pm 63$	$2317 \pm 81$
even	2515	581	$3112 \pm 80$	$2838 \pm 95$
Total	4346	837	$5160 \pm 100$	$5155 \pm 125$

followed by a  $j$ -prong second interaction were determined by combining the data on nearest secondary interaction induced by charged and neutrals with the normalization  $\sum_{i+j}^{\text{even}} \alpha_{ij} = 1$ . Any double scattering event with multiplicity  $(i+j-1)$  contributes a fraction  $\alpha_{ij} M_{i+j-1}$  to  $i$ -prong first interaction and so the total contribution to the  $i$ -prong first interaction from all double-scattering events is  $\sum_j^{\text{even}} \alpha_{ij} M_{i+j-1}$ .

In order to perform the model calculation we need the number of one-prong pn

and two-prong pd events. Following a spectator model of pd collisions, we have

$$P_2(\text{pd}) = 0.5[P_1(\text{pn}) + P_2(\text{pp})],$$

where  $P_N(\text{hx}) = \sigma_N(\text{hx})/\sigma_{\text{inel}}(\text{hx})$  is the probability of an inelastic  $N$ -prong hx collision. We also note that on the basis of isospin and factorization arguments, one-prong inelastic pn cross section may be estimated by

$$P_1(\text{pn}) = (0.6 \pm 0.1)P_2(\text{pp}).$$

Our evaluation of  $P_2(\text{pp})$  from the values of cross sections  $\sigma_2(\text{pp})$  and  $\sigma_{\text{inel}}(\text{pp})$  at 400 GeV/c from the data of Ref. [1] yields the values for the number of one-prong pn events as  $120 \pm 15$  and two-prong pd events as  $200 \pm 21$ . The number of neutrals at each multiplicity calculated on the basis of assumption (1) are added to the respective primary multiplicity.

The secondary interactions due to charged particles and the interactions induced by neutrals are measured on the scanning table. In total we have measured 1523 secondary interactions induced by charged prongs from events in the fiducial volume. Since some

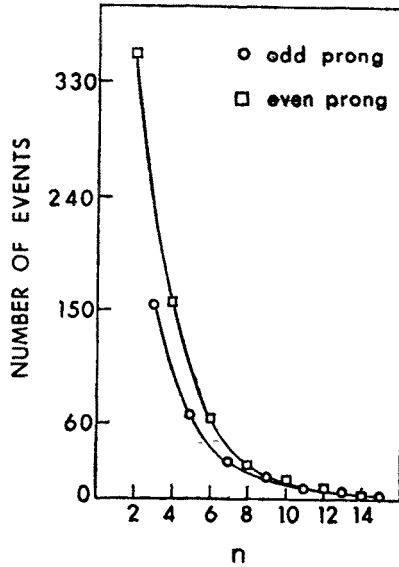


Fig. 2. Multiplicity ( $n$ ) distribution of nearest secondary interactions (curve drawn to guide the eye)

of the events are associated with more than one secondary interactions, and since we are interested in finding the characteristics for second scatter events from this data, we take into account only the nearest secondary interaction off a primary event. To this we have added the number of close secondaries determined earlier to effect the correction to the multiplicity distribution in Table I. Our sample consists of 914 secondary interactions in this category. The multiplicity distribution of these events shown in Fig. 2 is heavily peaked at low multiplicity. In this sample there are 288 odd-prong and 626

even-prong secondary events. The number of two-prong events in this category is 352. The distribution of the number of nearest even- and odd-pronged secondary events with primary multiplicity is given in Table II.

TABLE II

Distribution of secondary events (even- and odd-prong) w.r.t. primary multiplicity

Primary multiplicity $N_{eq}$	No. of nearest secondary events	
	even-prong	odd-prong
3	13	7
4	37	18
5	24	21
6	38	23
7	56	34
8	61	27
9	56	27
10	59	31
11	54	15
12	54	22
13	38	18
14	37	7
15	18	8
16	25	11
17	22	2
18	8	6
19	8	4
20	8	1
21	5	2
22	2	2
23	0	1
24	2	1
25	0	0
26	1	0

From figure 2 and Table II we observe that the ratio of the number of secondary events with even-charged prongs to that of primary events with odd-charged prongs is much larger than the ratio of the number of secondary events with odd-charged prongs to that of primary events with even-charged prongs. We also find that the ratio of the number of secondary events with even-charged-prongs to that of primary events with even-charged-prongs is much higher than the ratio of the number of secondary events with odd-charged-prongs to that of the primary events with odd-charged-prongs. This observation indicates that an even-prong secondary interaction is always more probable irrespective of whether the first interaction multiplicity is odd or even. This has an important bearing on the method of separation of the double scatter events into initial pn and pp interactions. Conditions in this experiment would suggest that an even-prong secondary interaction off an odd- (or even-) prong primary represent an initial pn (or pp)

interaction followed by an interaction induced by a charged (or neutral) particle on the nuclear proton (or neutron). We determine the number of initial pn (or pp) events in the even-prong sample by the procedure described below.

We obtain the ratio of the total number of even-prong secondary interactions to the total number of odd-prong primary interactions to be  $0.126 \pm 0.004$ . To determine the ratio of the number of even-prong interactions induced by neutrals to the total number of even-prong primary interactions, we use our measured 986 neutral decay and interactions induced by neutrals from events in the fiducial volume. This number reduces to  $626 \pm 17$  by the combined effect of (i) exclusion of decays or interactions other than the first and (ii) inclusion of those events obtained above for correcting the detection probabilities as in Table I. Out of these, 297 events belonged to primary events with even-charged-prong and 329 belonged to those with odd-charged-prong. We assume that two-pronged events arise due to either neutral and strange decays or  $\gamma$ -conversions, and a fraction of three-prong events are due to a  $\gamma$ -conversion in the field of an atomic electron. We are then left with  $86 \pm 7$  interactions induced by neutrals in our sample. The distribution of these events among odd- and even-prong primary interactions is given in Table III.

TABLE III

Distribution of interactions ( $n > 2$ ) induced by neutrals with respect to primary multiplicity

Primary multiplicity	No. of interactions induced by neutrals with	
	odd-charged prong	even-charged prong
odd	27	13
even	33	13

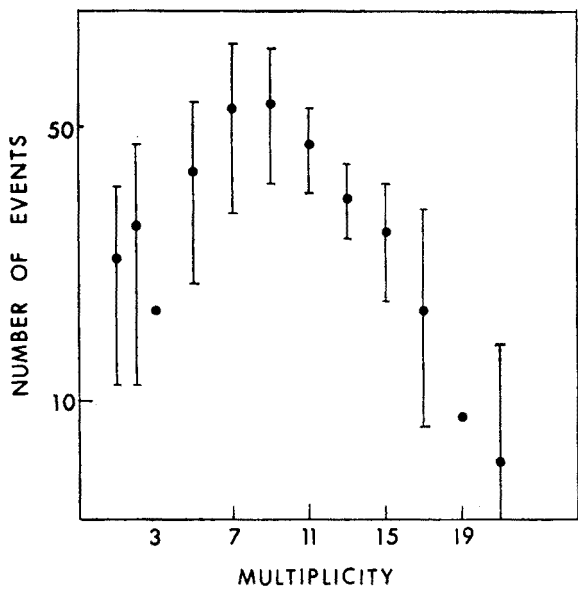


Fig. 3. First interaction multiplicity distribution of the double scattered events (see text)

TABLE IV

pn and pp multiplicity distribution after correcting for double scattering in pd interactions at 400 GeV/c

$N_{ch}$	pn interaction	pp interaction
1	$143 \pm 19$	
2		$228 \pm 27$
3	$364 \pm 34$	
4		$313 \pm 34$
5	$414 \pm 38$	
6		$414 \pm 36$
7	$460 \pm 43$	
8		$454 \pm 38$
9	$441 \pm 40$	
10		$386 \pm 34$
11	$356 \pm 33$	
12		$310 \pm 30$
13	$236 \pm 27$	
14		$230 \pm 27$
15	$165 \pm 20$	
16		$110 \pm 18$
17	$97 \pm 16$	
18		$78 \pm 16$
19	$50 \pm 11$	
20		$46 \pm 13$
21	$30 \pm 10$	
22		$26 \pm 9$
23	$6 \pm 2$	
24		$11 \pm 3$
25	$6 \pm 2$	
26		$2 \pm 1$
27	$1 \pm 1$	
28		$1 \pm 1$
Total	$2769 \pm 96$	$2639 \pm 91$

The error in the number of interactions induced by neutrals represent the uncertainty of assigning an event to a given primary interaction where there are more than one such interaction in the frame, combined with systematic uncertainty.

The charged multiplicity dependence of the resulting fraction of double scattered events calculated from the data summarised in Tables II and III is then utilized to calculate the number of double scattered events at each even topology. These are then separated from the even prong sample. The overall average fraction of double scattered events in the even prong sample of our data amounted to  $0.128 \pm 0.011$ . The final result is practically insensitive to the exclusion of neutral induced interactions from the data, except the contribution to the two-prong sample. This is because most of the neutral interactions (charged  $n \geq 3$ ) observed in the frames could be assigned only to interactions much ahead of the fiducial line and outside the field of view. The values of  $\alpha$ 's for  $i = 1, 2$  were not measured in this experiment and were assessed from backward extrapolation of the mea-

sured probabilities. The first interaction multiplicity distribution obtained by this method is shown in Fig. 3. The fraction of pd events which occur off neutron calculated from our final results is  $0.52 \pm 0.02$ . This compares fairly well with the result  $0.51 \pm 0.01$  from counter experiment [7] which measured  $\sigma_T(pn)$  and  $\sigma_T(pp)$ . The resulting pn and pp multiplicity distributions are given in Table IV shown in Fig. 4.

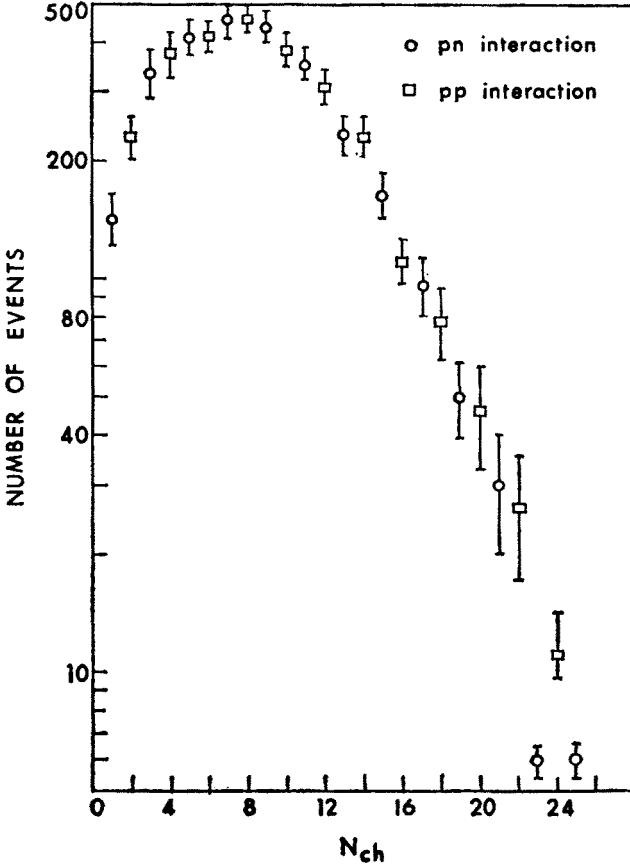


Fig. 4. pn and pp multiplicity distribution from pd interaction at 400 GeV/c (data corrected for double scattering)

The average first-interaction-multiplicity of double scattered events is  $9.46 \pm 0.14$ . We find from Fig. 3 that there is a substantial rise in contribution up to  $\sim$  average multiplicity. This means that the product of an initial pn interaction has a probability to interact with the second nucleon and this increases with first-interaction-multiplicity up to the average.

We have evaluated the contribution to the first interaction topology using Eq. (2a) of Ref. [2] by adjusting the free parameter  $\alpha$  and using  $n_0 = n_-$  for pp interactions and



$n_0 = n_- + 1$  for pn interactions with the normalisation  $\sum_{i=1}^{28} P_i = 1$ . The best  $\chi^2$  obtained is 1.52/d.o.f. with  $\alpha = 0.027 \pm 0.005$  showing that the model and our data are not incompatible.

### 3. Results and discussion

Tables V and VI list the moments [3] and statistical parameters which characterize the pn and pp charged multiplicity distributions in the momentum range 100–400 GeV/c. The comparison should be made with some precautions because somewhat different approaches are followed in deriving pn distributions at different energies. At 100 GeV/c

TABLE V

Properties of pn multiplicity distribution at 400 GeV/c and comparison with those at other energies  
(all these distributions are derived from pd experiments)

	100 GeV (Ref. [4])	195 GeV* (Ref. [5])	200 GeV* (Ref. [6])	300 GeV* (Ref. [2])	400 GeV* Present work
$\langle N \rangle$	$6.19 \pm 0.12$	$7.71 \pm 0.13$	$7.11 \pm 0.12$	$7.84 \pm 0.17$	$8.48 \pm 0.10$
$D$	$3.37 \pm 0.08$	$4.08 \pm 0.09$	$3.62 \pm 0.07$	$4.41 \pm 0.06$	$4.64 \pm 0.08$
$\langle N \rangle / D$	$1.83 \pm 0.05$	$1.88 \pm 0.05$	$1.96 \pm 0.06$	$1.77 \pm 0.07$	$1.82 \pm 0.04$
$\gamma_1$	$0.67 \pm 0.06$	$0.62 \pm 0.06$	$0.87 \pm 0.05$	$0.61 \pm 0.06$	$0.58 \pm 0.04$
$\gamma_2$	$3.57 \pm 0.14$	$3.33 \pm 0.21$	$4.92 \pm 0.18$	$3.20 \pm 0.20$	$3.06 \pm 0.17$
$M_0$	$5.06 \pm 0.24$	$6.44 \pm 0.32$	$5.53 \pm 0.24$	$6.49 \pm 0.25$	$7.13 \pm 0.21$
$M_0 / \langle N \rangle$	$0.81 \pm 0.05$	$0.83 \pm 0.07$	$0.77 \pm 0.06$	$0.82 \pm 0.04$	$0.84 \pm 0.02$

\* Data corrected for double scattering within deuterium (see text).

TABLE VI

Properties of pp multiplicity distribution as derived from pd data at 400 GeV/c and comparison of these with the values from proton target experiments at energies from 100–405 GeV/c

	100 GeV (Ref. [8])	102 GeV (Ref. [7])	205 GeV (Ref. [9])	300 GeV (Ref. [10])	405 GeV (Ref. [1])	400 GeV Present work
$\langle N \rangle$	$6.49 \pm 0.11$	$6.31 \pm 0.07$	$7.67 \pm 0.07$	$8.49 \pm 0.15$	$8.97 \pm 0.13$	$8.99 \pm 0.12$
$D$	$3.28 \pm 0.06$	$3.12 \pm 0.04$	$3.82 \pm 0.04$	$4.23 \pm 0.10$	$4.74 \pm 0.08$	$4.68 \pm 0.07$
$\langle N \rangle / D$	$1.98 \pm 0.05$	$2.02 \pm 0.03$	$2.01 \pm 0.08$	$2.00 \pm 0.05$	$1.89 \pm 0.05$	$1.92 \pm 0.03$
$\gamma_1$	$0.67 \pm 0.04$	$0.65 \pm 0.03$	$0.65 \pm 0.03$	$0.65 \pm 0.05$	$0.75 \pm 0.05$	$0.63 \pm 0.04$
$\gamma_2$	$3.19 \pm 0.17$	$3.18 \pm 0.12$	$3.24 \pm 0.10$	$3.31 \pm 0.15$	$3.64 \pm 0.22$	$3.16 \pm 0.14$
$M_0$	$5.14 \pm 0.22$	$4.83 \pm 0.02$	$5.91 \pm 0.03$	$7.11 \pm 0.65$	$7.73 \pm 0.41$	$7.51 \pm 0.22$
$M_0 / \langle N \rangle$	$0.79 \pm 0.03$	$0.76 \pm 0.02$	$0.77 \pm 0.03$	$0.83 \pm 0.03$	$0.86 \pm 0.04$	$0.83 \pm 0.02$

Lys et al. [4] considered the screening and rescattering as independent of multiplicity and derived the pn distributions from the odd prong data under a no cascade mode. Eisenberg et al. [5] at 195 GeV/c employed a moderate cascading formulation while Sheng et al. [2]

at 300 GeV/c effected correction for double scattering by assuming that the multiplicity distribution of second scatter events is the same as that of the secondary interactions independent of primary multiplicity. At both these energies no correction has been made for slow-proton detectability bias. At 200 GeV/c Dombeck et al. [6] employed two different models for double scattering and reported that either model gives a satisfactory description of data. However, the pn distribution reported by them was extracted with the assumption that the multiplicity of negatives produced in the second interaction follows a Poisson distribution. At all these energies, no correction, though expected to be small, has been made for deuteron-final-state and wave function symmetry effects.

Fig. 5 shows that the deviation from the constant  $\langle N \rangle / D$  ( $\sim 2$  from results of experiments with doubly charged or neutral initial states). Our analysis further reduces the deviation at its maximum e.g. at 405 GeV/c. If the fluctuations in the value of  $\langle N \rangle / D$  for pn interactions are assumed to be caused by inaccuracy in the assessment of one prong contribution, then the results show a probable constancy around a significantly lower value.

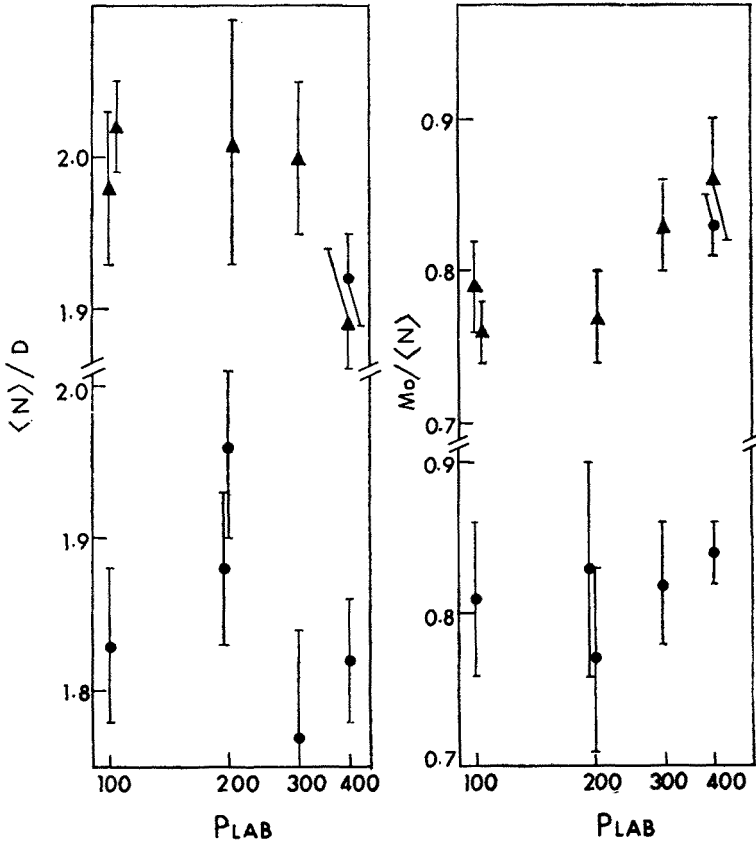


Fig. 5. Momentum dependence of  $\langle N \rangle / D$  (left) and  $M_0 / \langle N \rangle$  (right) for pp (upper) and pn (lower) distributions. All pn distributions are derived from pd experiments. 400 GeV pp point is obtained from present work. The symbol (▲) shows the values obtained from HBC experiments

The skewness  $\gamma_1$  of the pp (except for 405 GeV/c value where it is about 2 s.d. away) and pn (except for 200 GeV/c value where it is  $\sim 5$  s.d. away) show constancy in the range 0.6–0.65. While the “excess” ( $\gamma_2 - 3$ ) for pp distributions in the momentum range maintains a constant value close to but consistently different from the normal, its value for pn distributions maintains a downward trend and takes a value very close to it.

The parameter  $M_0/\langle N \rangle$  for both pn and pp distributions over the momentum range, however, shows a similarity of being less dependent on beam energy with a mean value (of course with large errors) about 0.8. Since this parameter is more dependent on the central features of the distribution where the confidence of data is high, we conclude that it gives a better assessment of the probability distribution. The momentum independence of  $M_0/\langle N \rangle$  also fulfils the requirement of KNO scaling.

We express our deep gratitude to Dr. C. T. Murphy and Dr. H. B. White Jr. of Fermilab for providing us the films on loan. We also thank our colleagues and scanning staffs at our laboratory for their careful and painstaking work of scanning.

#### REFERENCES

- [1] C. Bromberg et al., *Phys. Rev. Lett.* **31**, 1563 (1973).
- [2] A. Sheng et al., *Phys. Rev.* **D11**, 1733 (1975).
- [3] The four moments of distribution are the mean charged multiplicity  $\langle N \rangle$ , the dispersion  $D$ , the skewness  $\gamma_1$  and the kurtosis  $\gamma_2$ . The other parameters are the mode  $M_0$ ,  $\langle N \rangle/D$  and  $M_0/\langle N \rangle$ .
- [4] J. E. A. Lys et al., *Phys. Rev.* **D16**, 3127 (1977).
- [5] Y. Eisenberg et al., *Phys. Lett.* **60B**, 305 (1976).
- [6] T. Dombeck et al., *Phys. Rev.* **D12**, 86 (1978).
- [7] A. S. Carroll et al., *Phys. Rev. Lett.* **33**, 928 (1974).
- [8] J. Erwin et al., *Phys. Rev. Lett.* **32**, 234 (1974).
- [9] S. J. Barish et al., *Phys. Rev.* **D9**, 2689 (1974).
- [10] A. Firestone et al., *Phys. Rev.* **D10**, 2080 (1974).